Orthogonal Multicarrier Division Duplexing for Point-to-Point Communications

Wenxun Qiu, Hlaing Minn
University of Texas at Dallas, Richardson, TX, USA

Abstract—**Traditional communication systems adopt either time division duplexing (TDD) or frequency division duplexing (FDD). TDD requires guard interval and FDD needs guard band. Orthogonal multicarrier division duplexing (MDD) is a new duplexing scheme, which can avoid both guard interval and guard band. In this paper, we propose a new MDD scheme with a group-wise subcarrier partition, which is more robust to the inter-carrier interference (ICI) than the subcarrier-wise scheme, while keeping the same or better outage performance. We introduce somewhat modified block outage probability and block outage capacity metrics which are defined in such a way to facilitate the analysis and design of duplexing schemes in point-to-point (P2P) system. We give the closed-form of the block outage probability and derive the maximal capturable frequency diversity order based on outage probability. By analysis and simulation, it is verified that in P2P system, the proposed MDD scheme outperforms the existing schemes.**

I. Introduction

In communication systems, the signals from different transmitters should be separated from each other by some mechanisms so that the signals can be appropriately recovered. A fundamental approach is to enforce the orthogonality of the signals from different transmitters. There are several ways in which we can isolate the different signals. Typically, we can have time division duplexing (TDD) in time domain and frequency division duplexing (FDD) in frequency domain.

For P2P and point-to-multipoint (P2M) communications, TDD and FDD are two widely adopted duplexing schemes. [1] and [2] have listed the advantages and disadvantages of both schemes. FDD can achieve full duplexing, however, a guard band is required between uplink (UL) and downlink (DL) in order to limit the interference between them. For transmission schemes which require channel state information (CSI), FDD needs explicit CSI feedback. On the other hand, TDD can enjoy better frequency diversity without wasting any guard band, and the CSI can be obtained by channel reciprocity without requiring explicit feedback. However, since TDD is not full duplexing in a strict sense, the CSI has some inevitable delay. Moreover, TDD requires more stringent synchronization and a guard interval to absorb propagation delays and maintain the orthogonality. In general, if the coverage of the system is large, FDD systems outperform TDD systems, while TDD is preferred for small coverage areas.

Orthogonal frequency division multiplex (OFDM) system is adopted by many broadband systems, e.g. 802.11a, LTE, etc, due to its low equalizer complexity in frequency-selective fading channel and better resource granularity for adaptation. Conventionally, UL and DL signals maintain orthogonality of the user signals in their respective links. Between UL and DL, the signals are separated by a large guard band in FDD or guard interval in TDD. For P2P system, [3] and [4] proposed a duplexing scheme, respectively called orthogonal division duplexing (ODD) or orthogonal frequency division duplexing (OFDD), which keeps the signals from both transceivers orthogonal. With that scheme, both the guard band in FDD and the guard interval in TDD can be avoided. The existing ODD scheme in [3] and [4] uses subcarrier-wise interleaved subcarrier partitioning between UL and DL, and hence it is not robust to ICI (e.g., caused by carrier frequency offset (CFO)). Further, [5] proposed a scheme to solve the large dynamic range problem, and [6] applies a combination of ODD and FDD to cellular systems. However, in these papers, the implementation issue has not well addressed, and the advantages and disadvantages of ODD have not been thoroughly analyzed except presenting simulation results. The lack of analytical performance metric limits further insights into the characteristics of the scheme, as well as the design and optimization. In this paper, we consider a more general orthogonal multicarrier division duplexing (denoted as MDD in the rest) in P2P systems, where other subcarrier partitioning schemes are also allowed. The spectral occupancies of three duplexing schemes are shown in Fig. 1. For the proposed MDD, we form groups of subcarriers and interleave them over the whole frequency band. By grouping the subcarriers, the system can be more robust to the CFO without sacrificing the frequency diversity. Moreover, in MDD, CSI can be obtained by the channel reciprocity with appropriately located pilots (e.g. [12]).

The contributions of this paper are summarized as follows:

- We propose a new MDD scheme for P2P systems with a group-wise subcarrier partitioning between UL and DL based on the block outage probability analysis. The group-wise scheme can achieve full frequency diversity while sustaining better robustness to the ICI. The implementation issues are also analyzed.
- We introduce somewhat modified block outage probability and outage capacity to analyze the performance of several duplexing schemes. They can be viewed as performance metrics based on packet level which is practically more meaningful. The effectiveness of this approach is justified and the closed-form solution of outage probability is provided.

The rest of this paper is organized as below. Section II presents

978-1-4577-2053-6/12/$31.00 ©2012 IEEE

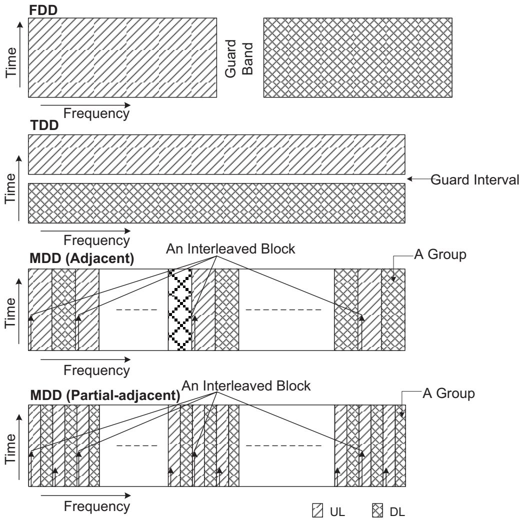

Fig. 1. Comparison of different duplexing schemes

the concept of MDD. In addition, the block outage probability and capacity are introduced to analyze the duplexing schemes, and a subcarrier partitioning between UL and DL is proposed based on the analysis. In Section III, performance comparison with existing schemes is given. Finally, the conclusion is given in Section IV.

II. Orthogonal Multicarrier Division Duplexing

In OFDM systems, all the subcarriers are orthogonal within each link. But considering UL and DL, these two links are isolated by guard band in FDD or guard interval in TDD, which is a waste of the resource. The fundamental idea of MDD is based on OFDM principle with UL and DL occupying different subcarriers of the same OFDM systems. A simple way to explain MDD is to view UL and DL as two users sharing the whole bandwidth in an OFDMA system. The difference is that their transmissions are in opposite directions, i.e., the two terminals communicate with each other simultaneously. And we should keep the combined signals orthogonal at both terminals. Different from conventional OFDM systems, the frequency span of the DFT covers all the subcarriers of both UL and DL. Due to the orthogonality, the full duplexing can be achieved without sacrificing the big guard band as required in FDD systems. On the other hand, since MDD can distinguish different links in frequency domain, the guard interval in TDD can also be avoided. The frequency resource can be allocated to UL or DL flexibly. Thus, both UL and DL can enjoy more frequency diversity than FDD. And the transmission in MDD is continuous, which means the latency in MDD can be controlled better than in TDD.

A. Implementation

There are some implementation issues in MDD. The orthogonality in MDD requires stringent timing synchronization similar to TDD systems so that the two terminals can start each transmission simultaneously. To keep the orthogonality of the UL and DL signals at the both sides, the duration of CP in MDD should be larger than the propagation time (including delay spread), which is larger than the CP length in traditional OFDM systems. From this perspective, MDD is more suitable to small coverage area; or a smaller subcarrier spacing (i.e. a longer symbol duration) can be used to reduce the CP overhead ratio. In practice, we also need to assure that the received signal power is at least comparable to the leakage power from transmitter at the same radio. Thus, the attenuation by the isolator between transmitter and receiver should be no less than the path loss attenuation. This requirement leads to small communication range again. For example, if the isolator attenuation is 85dB [7], the communication range can be around 210m when we apply the path loss of the micro cell line-of-sight scenario [8]. Typically, indoor wireless systems can be potentially a good application of MDD. Therefore, we consider the quasi-static frequency-selective channel in this paper. In outdoor mobile environments, the frame duration can be appropriately set up so that the channel remains static within the frame duration.

Further, MDD can be adapted for multiple access systems with a small coverage range; while for a large coverage range, it may need some additional technical solution to deal with the large dynamic range problem, e.g., a analog filter bank is introduced to solve the large dynamic range problem in [5]. Since we focus on P2P system in this paper, this issue is not a concern here.

B. Outage Probability and Outage Capacity Analysis

In order to derive an advanced subcarrier partition scheme between UL and DL and compare different schemes in multicarrier systems, block outage probability and capacity in a repetition diversity channel[1] [9] are introduced. Each block here can be considered as a data packet. Within a block, the goal is to capture diversity and enhance outage performance. Additional motivation for considering block-wise performance is that, if the system applies ARQ schemes at block level, the throughput performance can be improved. In this section, we first provide the closed-form of probability density function (PDF) of the block mutual information and outage probability.

We assume there are $N_{\rm B}$ blocks for each terminal in one OFDM symbol, while each block contains M subcarriers. And all the blocks have the same structure. We consider a frequency-selective Rayleigh fading channel with discrete time channel impulse response vector $\mathbf{h}$ of the size $L_0 \times 1$ and covariance matrix $\mathbf{C_h} = \mathbb{E}[\mathbf{h}\mathbf{h}^H]$. We assume that the channel taps are uncorrelated and hence $\mathbf{C_h}$ is diagonal matrix. Assuming the subcarrier index as q, we denote the channel gains for the subcarriers belonging to ith block (whose tone indexes are denoted by $\mathbf{B}_i$) as $\{H_q, q \in \mathbf{B}_i\} = \{H_{\mathbf{B}_i}(1), ..., H_{\mathbf{B}_i}(M)\}^T = \mathbf{H}_{\mathbf{B}_i}$. Then we can define the mutual information of the block corresponding to $\mathbf{B}_i$ in a repetition diversity channel as [9]

[1]The use of repetitive coding is only for analytical tractability in assessing frequency diversity. Practical coding schemes (such as convolutional codes or Turbo codes) across frequency domain can capture the frequency diversity revealed by the repetitive coding.

$$I_B(i) = \log_2(1 + \gamma \sum_{m=1}^{M} |H_{\mathbf{B}_i}(m)|^2). \quad (1)$$

Here, γ is the SNR. The correlation matrix of $\mathbf{H}_{\mathbf{B}i}$ is

$$\mathbf{C}_{\mathbf{H}i} = \mathbb{E}[\mathbf{H}_{\mathbf{B}i}\mathbf{H}_{\mathbf{B}i}^H] = \mathbf{V}\boldsymbol{\Sigma}\mathbf{V}^H = \mathbf{U}\mathbf{U}^H, \quad (2)$$

where $\mathbf{U} = \mathbf{V}\boldsymbol{\Sigma}^{1/2}$, $\mathbf{V}$ is a unitary matrix and $\boldsymbol{\Sigma}$ is a diagonal matrix of ordered eigenvalues $\{\lambda_l\}$. Thus, for a multipath Rayleigh fading channel, we can have $\mathbf{H}_{\mathbf{B}i} = \mathbf{U}\tilde{\mathbf{H}}_{\mathbf{B}_i}$, where $\tilde{\mathbf{H}}_{\mathbf{B}_i}$ is a zero-mean complex Gaussian random vector with the covariance matrix $\mathbf{I}_M$ (the $M \times M$ identity matrix). Then we have the total channel energy for block i as

$$Z_i \triangleq \sum_{m=1}^{M} |H_{B_i}(m)|^2 = \sum_{l=1}^{K} \lambda_l |\tilde{\mathbf{H}}_{\mathbf{B}_i}(l)|^2, \quad (3)$$

where K is the number of non-zero eigenvalues.

Theorem 1: If all the blocks have the same structure, $\{Z_i, \forall i\}$ have the same PDF.

Proof: Since all the blocks have the same structure, the index set $\mathbf{B}_i$ can be obtained by shifting $\mathbf{B}_0$ by M_i subcarriers, as $\mathbf{B}_i = \mathbf{B}_0 + M_i$. Then we have

$$\mathbf{H}_{\mathbf{B}i} = \mathbf{F}_{\mathbf{B}i}\mathbf{h} = \mathbf{F}_{\mathbf{B}0}\boldsymbol{\Lambda}_i\mathbf{h} \quad (4)$$

where $\boldsymbol{\Lambda}_i \triangleq \mathrm{diag}\{1, e^{-\frac{j2\pi M_i}{N_\mathrm{F}}}, e^{-\frac{j2\pi 2M_i}{N_\mathrm{F}}}, \cdots, e^{-\frac{j2\pi(L_0-1)M_i}{N_\mathrm{F}}}\}$, and $\mathbf{F}_{\mathbf{B}i}$ is a submatrix of $N_\mathrm{F} \times N_\mathrm{F}$ DFT matrix constructed by taking the rows corresponding to tone indexes in $\mathbf{B}_i$ and the first L_0 columns. Then we have

$$\mathbf{C}_{\mathbf{H}i} = \mathbf{F}_{\mathbf{B}0}\boldsymbol{\Lambda}_i\mathbf{C}_\mathbf{h}\boldsymbol{\Lambda}_i^H\mathbf{F}_{\mathbf{B}0}^H. \quad (5)$$

Since all channel taps are mutually independent, $\mathbf{C}_\mathbf{h}$ is diagonal. Then $\mathbf{C}_{\mathbf{H}i} = \mathbf{C}_{\mathbf{H}0}$. Thus, different blocks have the same eigenvalue set $\{\lambda_l\}$. By (3), $\{Z_i, \forall i\}$ have the same PDF. □

By the analysis above, we can use one of the blocks to characterize the whole frequency band. Then we can adopt $I_B = I_B(i)$ to define the outage probability and capacity for the system following [9] as

$$P_\text{out} = P\{I_B(i) < R_\mathrm{T}\} = P\{I_B < R_\mathrm{T}\} \quad (6)$$

$$C_\text{out} = N_B \cdot \log_2(1 + \gamma G_Z^{-1}(1-\epsilon)). \quad (7)$$

Here, $G_Z(\cdot)$ is the complementary cumulative distribution function (CCDF) of Z_i and ϵ is the corresponding outage probability.

Following [10], we can have the pdf of Z_i. There are two cases as follows.

- CASE I: $\boldsymbol{\Sigma}$ has at least two distinct eigenvalues.

From [10], we can obtain the pdf of Z_i as

$$g_{Z_i}(z) = \sum_{l=1}^{M_e}\sum_{k=1}^{\kappa_l} A_{lk}\frac{1}{\lambda_l} f_{2k}(z/\lambda_l), \quad (8)$$

where M_e is the number of distinct non-zero eigenvalues, κ_l is the order of lth distinct non-zero eigenvalue, A_{lk} is defined in [10] (we omit it due to space limitation) and

$$f_n(x) = \frac{x^{n/2-1}e^{-x}}{\Gamma(n/2)}, 0 < x < \infty \quad (9)$$

where $\Gamma(\cdot)$ is the Gamma function. The CCDF of Z_i is

$$G_{Z_i}(z) = \mathbb{P}\{Z_i > z\} = \sum_{l=1}^{M_e}\sum_{k=1}^{\kappa_l} \frac{A_{lk}}{\Gamma(k)\lambda_l^k} \sum_{v=0}^{k-1} e^{-z/\lambda_l} \frac{(k-1)!}{v!} z^v \lambda_l^{k-v}. \quad (10)$$

We have a special case in CASE I that all the non-zero eigenvalues of Σ are distinct. For this special case, we have the pdf of Z_i as

$$g_{Z_i}(z) = \Lambda \sum_{l=1}^{K} -a_l \exp(-z/\lambda_l), z \geq 0 \quad (11)$$

where $a_l = \prod_{k=1,k\neq l}^{K}\left(\frac{1}{\lambda_l} - \frac{1}{\lambda_k}\right)^{-1}$ and $\Lambda = \left\{\prod_{l=1}^{K}\frac{-1}{\lambda_l}\right\}$. The CCDF of Z_i is

$$G_{Z_i}(z) = \mathbb{P}\{Z_i > z\} = -\Lambda \sum_{l=1}^{K} a_l \lambda_l e^{-z/\lambda_l}, z \geq 0. \quad (12)$$

- CASE II: $\boldsymbol{\Sigma}$ has K identical non-zero eigenvalue λ.

The PDF of Z_i is

$$g_{Z_i}(z) = \frac{z^{K-1}}{\Gamma(K)\lambda^K} e^{-z/\lambda}, z \geq 0. \quad (13)$$

The CCDF of Z_i is

$$G_{Z_i}(z) = e^{-z/\lambda} \sum_{k=0}^{K-1} \frac{(K-1)!}{k!} \frac{z^k \lambda^{K-k}}{\Gamma(K)\lambda^K}, z \geq 0. \quad (14)$$

Then by (1), we have the pdf of I_B as

$$g_{I_B}(I) = \frac{2^I \ln 2}{\gamma} \cdot g_{Z_i}\left(\frac{2^I - 1}{\gamma}\right), I \geq 0. \quad (15)$$

Since the pdf of Z_i has two cases, correspondingly, the PDF of I_B and the outage probability also have two cases.

- CASE I: $\boldsymbol{\Sigma}$ has at least two distinct eigenvalues.

We have the PDF of I_B as

$$g_{I_B}(I) = \frac{2^I \ln 2}{\gamma} \cdot \sum_{l=1}^{M_e}\sum_{k=1}^{\kappa_l} A_{lk} \frac{1}{\lambda_l} \frac{(2^I-1)^{k-1} e^{-\frac{2^I-1}{\gamma\lambda_l}}}{(\gamma\lambda_l)^{k-1}\Gamma(k)}, \ I \geq 0.$$

Then we can obtain the outage probability as

$$P_\text{out}(R_\mathrm{T}, \gamma) = P\{I_B < R_\mathrm{T}\} = \int_0^{R_\mathrm{T}} g_{I_B}(I)\mathrm{d}I = \sum_{l=1}^{M_e}\sum_{k=1}^{\kappa_l} A_{lk}\left[1 - e^{-\frac{2^{R_T}-1}{\lambda_l\gamma}} \sum_{i=0}^{k-1} \frac{(2^{R_T}-1)^i}{i!}(\lambda_l\gamma)^{-i}\right]. \quad (16)$$

For the special case that all the non-zero eigenvalues are distinct, we have

$$g_{I_B}(I) = \frac{2^I \ln 2}{\gamma} \cdot \Lambda \sum_{l=1}^{K} -a_l \exp\left(\frac{-2^I+1}{\gamma\lambda_l}\right), I \geq 0, \quad (17)$$

$$P_\text{out} = \int_0^{R_\mathrm{T}} g_{I_B}(I)\mathrm{d}I = -\sum_{l=1}^{K} \Lambda a_l \lambda_l (1 - e^{-\frac{2^{R_\mathrm{T}}-1}{\lambda_l\gamma}}). \quad (18)$$

- CASE II: Σ has K identical non-zero eigenvalue λ.

We have the PDF of I_B as

$$g_{I_B}(I) = \frac{2^I \ln 2}{\gamma^K} \cdot \frac{(2^I-1)^{K-1}}{\Gamma(K)\lambda^K} e^{-\frac{2^I-1}{\gamma\lambda}}, I \geq 0, \quad (19)$$

and the outage probability as

$$P_\text{out} = \left[1 - e^{-\frac{2^R-1}{\lambda\gamma}} \sum_{k=0}^{K-1} \frac{(2^R-1)^k}{k!}(\lambda\gamma)^{-k}\right]. \quad (20)$$

For both cases, ϵ - outage capacity (outage capacity at the outage probability of ϵ) can be obtained by (7).

Theorem 2: The captured frequency diversity D_f is equal to the number of non-zero eigenvalues K of $\mathbf{C}_{\mathbf{H}i}$, and the maximal possible value of D_f is $D_{\mathrm{m}} = \min(L_0, M)$.

***Proof*:** Let us consider CASE II first. By Taylor expansion, we have $e^x = \sum_{k=0}^{\infty} \frac{x^k}{k!}$. By substituting it into (20), we have

$$P_{\mathrm{out}} = 1 - e^{-\frac{2^R-1}{\lambda\gamma}} \left[e^{\frac{2^R-1}{\lambda\gamma}} - \sum_{k=K}^{+\infty} \frac{(2^R-1)^k}{k!} (\lambda\gamma)^{-k} \right]$$

$$= e^{-\frac{2^R-1}{\lambda\gamma}} \sum_{k=K}^{+\infty} \frac{(2^R-1)^k}{k!} (\lambda\gamma)^{-k} \triangleq \Psi(\lambda\gamma) \quad (21)$$

In high SNR scenario, we can simplify (21) as

$$P_{\mathrm{out}} \approx e^{-\frac{2^R-1}{\lambda\gamma}} \frac{(2^R-1)^K}{K!} (\lambda\gamma)^{-K}. \quad (22)$$

Hence, for CASE II, the captured frequency diversity order is $D_f = K$.

For CASE I, denote the maximum and minimum eigenvalues by $\lambda_{\max}$ and $\lambda_{\min}$, respectively. Then by (3), we have

$$\sum_{l=1}^{M_e} \lambda_{\min} |\tilde{\mathbf{H}}_{B_i}(l)|^2 \le Z_i \le \sum_{l=1}^{M_e} \lambda_{\max} |\tilde{\mathbf{H}}_{B_i}(l)|^2. \quad (23)$$

which in turn yields

$$\Psi(\lambda_{\max}\gamma) < P_{\mathrm{out}} < \Psi(\lambda_{\min}\gamma) \quad (24)$$

For high SNR case, both the upper bound and the lower bound are of order K. Therefore, the captured frequency diversity order is K as well.

Since $\mathbf{C}_{\mathbf{h}}$ is diagonal full rank, from (2) we obtain

$$\mathrm{Rank}(\mathbf{C}_{\mathbf{H}i}) = \mathrm{Rank}(\mathbf{F}_{\mathbf{B}i}) = \min(L_0, M). \quad (25)$$

Consequently, we can have the maximal achievable frequency diversity as $D_m = \max(K) = \min(L_0, M)$. □

By the block outage probability analysis, we obtain the same conclusion (Theorem 2) as obtained by the traditional outage probability. It verifies the effectiveness of block outage probability. From Theorem 2, we have that the diversity order in high SNR scenario only depends on L_0 and M. For MDD system, UL and DL share the whole bandwidth, which is double of the bandwidth of each link in FDD system. Hence, the time resolution of MDD system is twice finer than FDD system. This feature gives MDD system more resolvable channel taps. If the channel has L_0 taps in MDD system, the corresponding channel in FDD system which occupies the same system bandwidth (each link occupies half of the whole bandwidth) would approximately have $L_0/2$ taps for rich scattering environments. Consequently, the MDD system has more capturable frequency diversity than FDD system. For TDD system, the capturable frequency diversity is the same as MDD system due to the same time resolution.

C. Subcarrier Partitioning between UL and DL

We can convert the subcarrier partitioning problem into the two steps. First, how to design the subcarrier block including block size M and its structure; second, how those subcarrier blocks form two links. According to Section II-B, in order to achieve the full frequency diversity we should have $M \ge L_0$. On the other hand, $M = L_0$ will provide larger multiplexing gain compared with the other cases of $M > L_0$ in a repetition diversity channel. Thus, we should have $M = L_0$.

The selection of subcarriers (block structure) cannot affect the frequency diversity order (c.f. Theorem 2). However, since different selection of subcarriers would impact the values of $\{\lambda_l\}$, the block outage probability is still related to the subcarrier selection or block structure. Consequently, another question arises that which block structure can achieve the best outage probability. We follow the classification in [13] to classify the block structure into 3 categories: band-type, interleaved-type and mixed-type. In band-type structure, all the subcarriers in one block are contiguously located, while in interleaved-type the subcarriers are uniformly spread out over the whole bandwidth. In the mixed structure, some subcarriers stick together as band type while the rest of the subcarriers are interleaved over the whole frequency band. Thus, if the number of interleaved subcarriers M_{intlv} out of M subcarriers of a block is zero, it represents a band-type block. When $M_{\mathrm{intlv}} = M$, it is an interleaved-type. A mixed-type corresponds to $0 < M_{\mathrm{intlv}} < M$. Fig. 2 shows outage probability

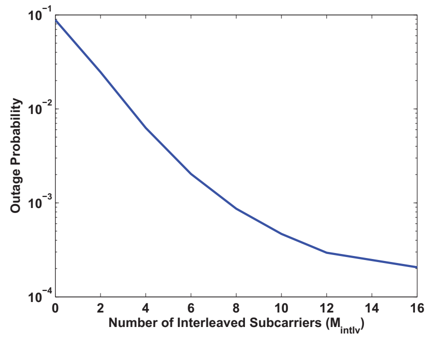

Fig. 2. Comparison of outage probability for different block structures

of different block structures with $M = 16$ in the system with $L_0 = 16$ (-1.5dB decay factor in the channel power delay profile (PDP)), $N_{\mathrm{F}} = 1024$. The performance becomes better when the number of interleaved subcarriers increases. And the interleaved-type structure has the best outage probability. This result matches our intuition.

Thus, the subcarrier partitioning between UL and DL should be such that each link is composed of several blocks each of which includes $M = L_0$ subcarriers which are uniformly interleaved over the whole band. For $\frac{N_{\mathrm{F}}}{2L_0}$ being an integer, we have $\mathbf{B}_0 = \{0, \frac{N_{\mathrm{F}}}{2L_0}, \frac{2N_{\mathrm{F}}}{2L_0}, \cdots, \frac{(L_0-1)N_{\mathrm{F}}}{2L_0}\}$.

The interleaved blocks forming one link have three styles: adjacent, partial-adjacent and non-adjacent. The subcarrier-wise partition scheme in [3] and [4] can be viewed as a non-adjacent style. And the other two styles are shown in the bottom two sub-figures of Fig. 1. Among them, adjacent style is the most robust to the ICI when considering the leakage from the transmitter to the receiver of the same radio. Let $\mathbf{J}_{\mathrm{R}}$ and $\mathbf{J}_{\mathrm{L}}$ represent the block index set for the received link and the leaked link, respectively. Then the subcarriers corresponding to each link are given as $\{q \in \mathbf{B}_l\}$, where $l \in \mathbf{J}_\mathrm{R}$ for the received link and $l \in \mathbf{J}_\mathrm{L}$ for the leaked link. The subcarrier partitioning becomes designing $\mathbf{J}_\mathrm{R}$ and $\mathbf{J}_\mathrm{L}$. The received signal on subcarrier $k \in \mathbf{J}_\mathrm{R}$ is

$$Y(k) = X(k)H_k S_0(0) + \sum_{q \in \mathbf{B}_l, q \neq k, l \in \mathbf{J}_\mathrm{R}} X(q) H_q S_0(q-k) + \sum_{q \in \mathbf{B}_l, l \in \mathbf{J}_\mathrm{L}} \beta X(q) S_1(q-k) + n_k, \tag{26}$$

where $X(q)$ denotes the transmitted modulation symbol on the qth subcarrier, β is the effective gain of the leaked link and n_k is an additive noise sample. The sequence $S_i(q-k)$ is the ICI coefficient between lth and kth subcarriers, which can be expressed as [11]

$$S_i(q-k) = \frac{\sin(\pi(q+\varepsilon_i - k))}{N \sin(\frac{\pi}{N}(q+\varepsilon_i-k))} e^{j\pi(1-\frac{1}{N})(q+\varepsilon_i-k)}, i = 0, 1.$$

Here, ε_0 and ε_1 are, respectively, the CFO of received link and leakage link normalized by the subcarrier spacing. In practice, CFO estimation and compensation are performed based on the received preamble and hence after that process the effective CFO for the received link will be negligible. Hence we just need to check the ICI power from the leaked link. With $\mathbb{E}[|X(q)|^2] = \sigma_x^2, q \in \mathbf{J}_\mathrm{L}$, the ICI power in received link caused by the leakage link is

$$P_\mathrm{ICI} = \sigma_x^2 \, |\beta|^2 \sum_{k \in \mathbf{B}_l, l \in \mathbf{J}_\mathrm{R}} \sum_{q \in \mathbf{B}_l, l \in \mathbf{J}_\mathrm{L}} |S_1(q-k)|^2. \tag{27}$$

From (27), the ICI power will be minimized if each link contains adjacent blocks, e.g., for symmetric links, $\mathbf{J}_\mathrm{R} = \{0, 1, \cdots, \frac{N_B}{2} - 1\}$ and $\mathbf{J}_\mathrm{L} = \{\frac{N_B}{2} \cdots, N_B\}$. In summary, the proposed subcarrier partitioning is such that each link has adjacent blocks while each block contains $M = L_0$ uniformly interleaved subcarriers. In another view, if we take the consecutive subcarriers as a group, the design is such that each link is composed of $N_G = L_0$ groups with $\frac{N_\mathrm{F}}{2L_0}$ consecutive subcarriers per group and these groups are uniformly interleaved across the band as in the third sub-figure of Fig. 1.

Compared with the scheme in [3] and [4] (which can be viewed as all blocks interleaving between UL and DL with optimal block structure or $N_G = N_\mathrm{F}/2$ groups for each link and each group with one subcarrier), our proposed scheme is more robust to the ICI without sacrificing outage probability performance. Furthermore, with well-located pilots (e.g., [12]), both UL and DL can estimate the channel of the whole bandwidth. Then by channel reciprocity, both terminals can have the channel knowledge of both links without any feedback. Since the transmission in MDD is continuous, the pilots can be inserted in any time slot according to the system requirement, This feature is significant since it provides better control of CSI delay, and hence better tracking and adaptation for the time-varying channel. (The pilot designs and channel estimation methods for the proposed scheme can be developed based on the existing literature (e.g., [12]), and are outside the scope of this paper.) However, in TDD, the delay of CSI cannot be avoided. To reduce that delay in TDD, we have to reduce the duration of each link, which would lead to frequent switching between DL and UL. The cost of guard interval and frame overhead consequently increases. Hence, MDD scheme has better feature in obtaining CSI and can adapt the channel more closely than TDD.

III. Simulation and Discussion

We consider the symmetric transmission where UL and DL occupy the same bandwidth. For FDD system, we assume that the bands for UL and DL are naturally separated. Then we do not consider extra guard band for FDD. Both UL and DL include 512 subcarriers and DFT size is $N_F = 512$. We use a multipath Rayleigh fading channel with $L_0 = 8$ independent taps having an exponential power delay profile (PDP) with 3dB per tap decay factor. For MDD system, we use the DFT size of $N_F = 1024$ and each link occupies 512 subcarriers. Since the time resolution of MDD is twice finer than FDD, we assume that the channel is with $L_0 = 16$ taps and -1.5 dB per tap decay PDP for MDD. And here we adopt $R_T = 2$.

The outage probability comparison is shown in Fig. 3, where E_b/N_0 denotes the energy over a block to noise spectral density ratio. In all the evaluation in this section, we adopt the structures achieving the best outage probability to calculate outage probability and capacity for different partitioning schemes (e.g., interleaved block structure for proposed scheme). For FDD system, both cases ($M = 8, 16$) have the same outage probability. Since $L_0 = 8$, when $M \geq L_0$ the captured frequency diversity is determined by L_0. This result is in line with Theorem 2. In MDD system, due to $L_0 = 16$, when $M < 16$, the captured frequency diversity is determined by M. And when $M \geq L_0$, the captured frequency diversity is L_0. Therefore, in MDD simulation, the case of $M = 16$ captures more frequency diversity than the case of $M = 8$. To show the performance for MDD with a non-optimal (in outage probability sense) block structure, we include a block structure consisting of uniformly interleaved $\frac{M}{2}$ subcarrier pairs where the two tones in each pair are separated by $\frac{N_\mathrm{F}}{2M}$ subcarriers. With our partitioning, this becomes an MDD scheme with $M = 16$ and $N_G = 8$. Performance degradation due to non-optimal block structure is observed as expected. Since ICI is excluded, the reference scheme in [3] and [4] achieves the same performance as the proposed MDD ($M = 16, N_G = 16$), and TDD. Both results verify the effectiveness of the proposed scheme. Additionally, the comparison of the interference caused by CFO with $\beta = 1$ and $\sigma_x^2 = 1$ is shown in Fig. 4. The proposed scheme ($N_G = L_0 = 16$) substantially outperforms

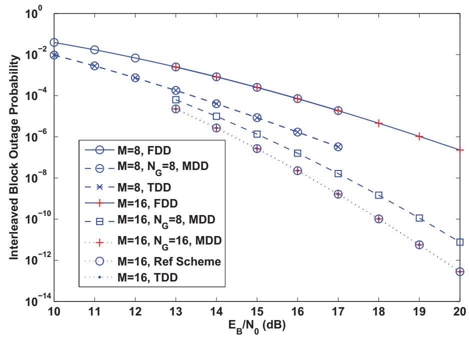

Fig. 3. Outage probability comparison of different duplexing schemes at $R_T = 2$ (ICI effect is excluded)

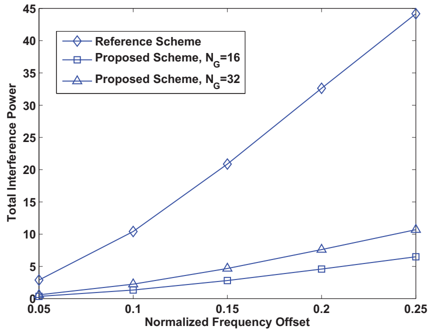

Fig. 4. The comparison of interference power caused by CFO

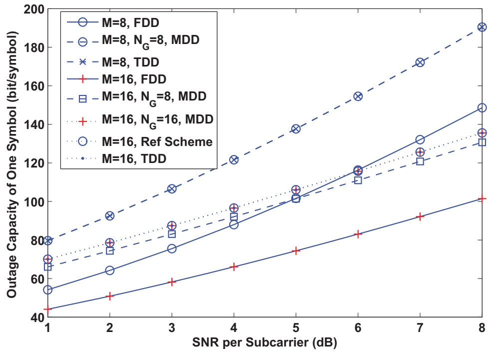

Fig. 5. Comparison of outage capacity per symbol for different duplexing schemes at $P_{\text{out}} = 10^{-4}$ (the effects of ICI and guard intervals are excluded)

the reference scheme in [3] and [4].

When compared to FDD, the proposed MDD scheme obviously outperforms FDD as shown in Fig. 3 and 5. The maximal capturable frequency diversity order of MDD is approximately double of FDD in rich scattering environments (c.f. Theorem 2). Additionally, due to different eigenvalues, we observe that in the cases of $M = 8$, the outage probabilities of MDD have better performance than FDD even at the same diversity order.

The outage capacity per symbol is shown in Fig. 5, where the MDD schemes also substantially outperform the FDD scheme with the same M. And the MDD scheme with $N_G = L_0$ is still one of the best schemes in the evaluation. TDD scheme has the same performance as the proposed scheme in outage probability and outage capacity, but here we do not count the guard interval and frame overhead which if incorporated will degrade the TDD system capacity. Further, as we mentioned in Section II-C, the MDD scheme has the advantage in obtaining CSI. Thus, comprehensively, the proposed MDD scheme also outperforms the TDD scheme. As a final comment, note that the proposed design minimizes the block outage probability while capturing maximum diversity order; but it can be tailored to the scenarios which require a smaller diversity order with a larger outage capacity (diversity-multiplexing trade-off [14]), e.g., see the results for MDD with $M = 16$ versus $M = 8$ in Fig. 5.

IV. Conclusion

We have presented a general orthogonal multicarrier division duplexing, which outperforms the existing duplexing schemes. We have introduced somewhat modified block outage probability/capacity to analyze different duplexing schemes in multicarrier systems. It is proven that if all subcarriers are divided into a set of blocks with the same structure, the pdf of mutual information for each block is the same. We also prove that the maximal capturable frequency diversity is determined by the rank of the effective channel correlation matrix. Based on the analysis, we find out that the subcarrier partition scheme can be derived from the block design. Consequently, we propose a new MDD scheme with group-wise subcarrier partitioning where the number of groups for each link is the same as the number of channel taps. The MDD scheme can avoid the guard interval and guard band. Moreover, the channel of both forward and reverse links can be obtained by appropriately designed pilots, and the delay of the channel information can be better controlled. Hence, the proposed MDD scheme is a promising transmission scheme for future systems.

References

[1] P. W.C. Chan, E. S. Lo, R. R. Wang and et al., "The evolution path of 4G networks: FDD or TDD?", *IEEE Commun. Mag.,* vol. 44, no. 12, Dec. 2006, pp. 42-50.

[2] E. Ayanoglu, M. Burgess, M. Pollack and A. Zamanian "Frequency Division Duplexing and Time Division Duplexing for Broadband Wireless Applications," *Broadband Wireless Internet Forum White Paper*, WP-3-TG-1, Feb. 28, 2001.

[3] D. Steer, K. Teo and B. Kirkland,"Novel method for communication using orthogonal division duplexing of signal (ODD)" *IEEE VTC*, vol. 1, Sep. 2002, pp. 381-385.

[4] R. Kimura and S. Shimamoto, "A multi-carrier based approach to wireless duplex: orthogonal frequency division duplex (OFDD)," *Intl. Symp. Wireless Commun. Systems*, pp. 368-372, 2006.

[5] R. Kimura and S. Shimamoto, "An Orthogonal Frequency Division Duplex (OFDD) System Using an Analog Filter Bank," *IEEE WCNC*, pp. 2275 - 2280, 2007.

[6] S. Lim, J. Lee, T. Kwon and D. Hong, "A new hybrid division duplex scheme: Orthogonal frequency division duplex (OFDD)," *IEEE MILCOM*, Oct. 2009, pp. 1 - 6.

[7] C.R Anderson, S. Krishnamoorthy, C.G. Ranson, and et al., "Antenna Isolation, Wideband Multipath Propagation Measurements, and Interference Mitigation for On-frequency Repeaters," *SoutheastCon, 2004. Proceedings. IEEE*, pp. 110 - 114, Mar. 2004.

[8] 3GPP, Technical Specification Group Radio Access Network, "Spatial channel model for Multiple Input Multiple Output (MIMO) simulations" (Relase 9), 3GPP TR 25.996 v9.0.0, Dec. 2009.

[9] G. Caire, G. Taricco and E. Biglieri, "Optimum power control over fading channels," *IEEE Trans. Info. Theory*, vol. 45, no. 5, July 1999.

[10] Y. Li, H. Minn and J. Zeng, "An average Cramer-Rao bound for frequency offset estimation in frequency-selective fading channels," *IEEE Trans. Wireless Commun.*, vol. 9, no. 3, Mar. 2010.

[11] Y. Zhao and S.-G. Häggman, "Intercarrier Interference Self-Cancellation Scheme for OFDM Mobile Communication Systems", *IEEE Trans. Commun*, vol. 49, no. 7, Jul. 2001, pp. 1185-1191.

[12] H. Minn and N. Al-Dhahir, "Optimal Training Signals for MIMO OFDM Channel Estimation", *IEEE Trans. Wireless Commun.*, vol. 5, no. 5, pp. 1158-1168, May 2006.

[13] W. Qiu, H. Minn and C.-C. Chong, "An Efficient Diversity Exploitation in Multiuser Time-Varying Frequency-Selective Fading Channels", *IEEE Trans. Commun.*, vol. 59, no. 8, pp. 2172 - 2184, Aug. 2011.

[14] L. Zheng, and D. N.C. Tse, "Diversity and multiplexing: a fundamental tradeoff in multiple-antenna channels", *IEEE Trans. Info. Theory*, vol. 49, no. 5, May 2003, pp.1073–1096.